

Fast Hip Joint Moment Estimation with A General Moment Feature Generation Method

Yuanwen Zhang, Jingfeng Xiong, Haolan Xian, Chuheng Chen, Xinxing Chen, Chenglong Fu, and Yuquan Leng

Abstract—The hip joint moment during walking is a crucial basis for hip exoskeleton control. Compared to generating assistive torque profiles based on gait estimation, estimating hip joint moment directly using hip joint angles offers advantages such as simplified sensing and adaptability to variable walking speeds. Existing methods that directly estimate moment from hip joint angles are mainly used for offline biomechanical estimation. However, they suffer from long computation time and lack of personalization, rendering them unsuitable for personalized control of hip exoskeletons. To address these challenges, this paper proposes a fast hip joint moment estimation method based on generalized moment features (GMF). The method first employs a GMF generator to learn a feature representation of joint moment, namely the proposed GMF, which is independent of individual differences. Subsequently, a GRU-based neural network with fast computational performance is trained to learn the mapping from the joint kinematics to the GMF. Finally, the predicted GMF is decoded into the joint moment with a GMF decoder. The joint estimation model is trained and tested on a dataset comprising 20 subjects under 28 walking speed conditions. Results show that the proposed method achieves a root mean square error of 0.1180 ± 0.0021 Nm/kg for subjects in test dataset, and the computation time per estimation using the employed GRU-based estimator is 1.3420 ± 0.0031 ms, significantly faster than mainstream neural network architectures, while maintaining comparable network accuracy. These promising results demonstrate that the proposed method enhances the accuracy and computational speed of joint moment estimation neural networks, with potential for guiding exoskeleton control.

Index Terms—Joint moment, kinetics estimation, lower-limb exoskeleton, deep learning

I. INTRODUCTION

LOWER-limb exoskeletons are capable of assisting in human locomotion, thus reducing joints moments, metabolic expenditure, and mechanical loading of joints. This allows it to be applied to assist weight-bearing workers, elderly individuals in need of walking assistance, and patients with arthritis [1], [2], [3], [4], [5]. During walking, the hip joint

contributes 40-50% of the total positive joint power of the lower limb joints [6], which means that hip-assisted walking exoskeletons can bring substantial benefits. Furthermore, compared with other lower limb exoskeletons, hip exoskeletons have smaller metabolic penalties caused by distal-borne mass [7]. Therefore, hip exoskeletons are considered an important choice for walking assistance.

The moment of the hip joint is an important basis for hip exoskeleton assistance. Since calculating joint moment with motion capture systems or force platforms is not feasible for real-world using of hip exoskeleton, it is necessary to utilize other sensors fixed on the exoskeleton system. Recent researchers have focused on determining the assistive torque of the exoskeleton based on the human motion information measured by these sensors, such as encoders on the motors or inertial measurement units (IMUs).

Currently, there are two main methods to generate the assistive torque of hip exoskeletons based on hip joint motion data: 1) determining output torque based on assistive torque curve generation and gait phase estimation, and 2) calculating assistive torque according to instantaneous joint moment estimates. The former method involves the following steps: a) estimating the gait phase and the assistive torque profile for the entire gait cycle based on the user's historical walking data, and b) generating the assistive torque based on the gait phase and the assistive torque profile [8], [9], [10]. However, this method may exhibit delayed assistive torque when dealing with variable walking gaits, which can hinder the user's movements. The other method generates assistive torque directly through a computational model by measuring the kinematic information of the human body [11], [12], [13]. Compared to the first method, the second method calculates assistive torque independent of gait periodicity, allowing it to generate appropriate walking assistance in real-time even with changing gaits. Therefore, joint moment estimates-based assistive torque calculation has the potential to become an important computational method for future exoskeleton control.

The estimation of hip biomechanical joint moment is most crucial in the instantaneous joint moment estimates-based method. However, it remains a significant challenge to estimate hip joint moment based on measurable data from the human body. Although some researchers have obtained joint moments by establishing approximate dynamic models [14], [15], these methods rely on complex sensor equipment such as plantar pressure sensors, which may decrease the stability of the exoskeleton system and reduce user comfort.

As data-driven methods have shown remarkable effectiveness in biological measurement and exoskeleton control fields

This work was supported in part by the National Natural Science Foundation of China under Grant 52175272 and Grant 62103180, in part by the Science, Technology and Innovation Commission of Shenzhen Municipality under Grant JCYJ20220530114809021, Grant KCXFZ20230731093059012, and Grant KCXFZ20230731093401004. (Yuanwen Zhang and Jingfeng Xiong contributed equally to this work.) (Corresponding authors: Yuquan Leng)

Yuanwen Zhang, Jingfeng Xiong, Haolan Xian, Chuheng Chen, Xinxing Chen, Chenglong Fu and Yuquan Leng are with the Shenzhen Key Laboratory of Biomimetic Robotics and Intelligent Systems and Guangdong Provincial Key Laboratory of Human-Augmentation and Rehabilitation Robotics in Universities, Southern University of Science and Technology, Shenzhen 518055, China, and also with the Department of Mechanical and Energy Engineering, Southern University of Science and Technology, Shenzhen 518055, China.

This work has been submitted to the IEEE for possible publication. Copyright may be transferred without notice, after which this version may no longer be accessible.

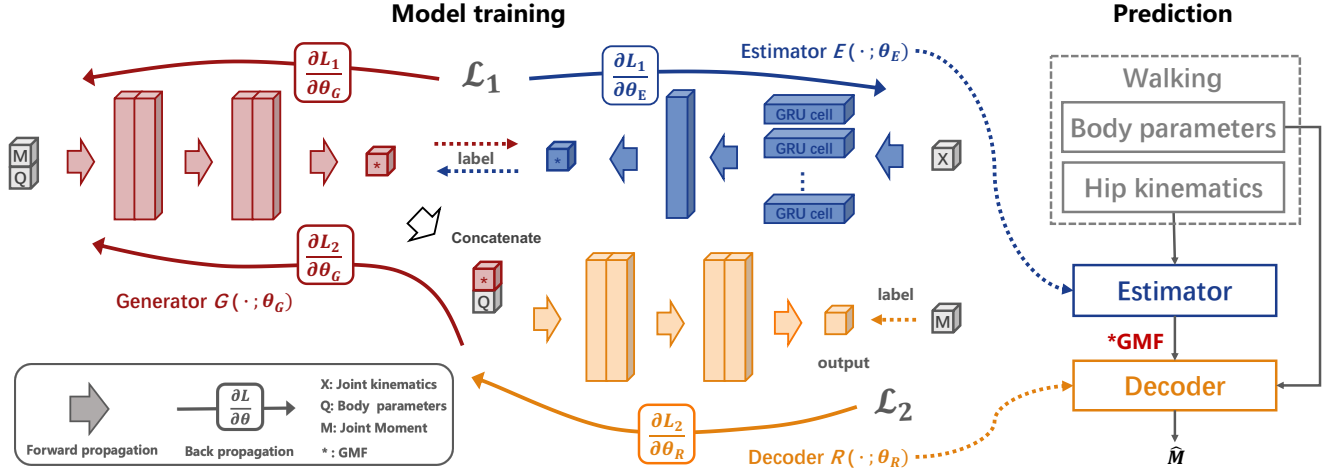


Fig. 1. The proposed method for fast hip joint moment estimation. During the training process, kinematic information (\mathbf{X}) is utilized as input for the estimator, while body parameters (\mathbf{Q}) and real joint moments (\mathbf{M}) serve as inputs for the generator. The decoder takes body parameters and the GMF generated by the generator (represented by “*”) as inputs. The trained model is then employed to estimate hip joint moments ($\hat{\mathbf{M}}$) during walking for new users. It is worth noting that the generator does not exist in the prediction process, and the input to the moment decoder comes from estimator, which is different compared to the training process.

[16], [17], [18], [19], researchers have started focused on measured motion information (such as hip joint position changes) by simple and lightweight sensors during human walking for the estimation of joint moment. Wang used the XGBoost method to achieve the prediction of the knee joint adduction moment in an experiment involving 106 participants by using only the information from two IMU sensors [20]. However, traditional machine learning methods have limited performance in improving prediction accuracy of joint moment estimation, and researchers are turning to neural networks to further enhance the prediction accuracy of joint moment. Molinaro trained a TCN network that utilized expanded causal convolutional layers to encode temporal information and learn data features from input, achieving hip joint moment prediction based on data of IMU and angle of hip joint [21], [22]. Furthermore, Hossain designed an Ensemble network that improved the performance of human dynamics prediction using deep neural network layers with different structure types. Through fusion modules and bagging techniques, the model achieved a more accurate prediction of lower-limb joint moment [23]. However, the aforementioned joint moment estimation methods, which are mainly used for offline biomechanical joint moment estimation, suffer from the problem of long computation time and lack of personalization, which leads to their inapplicability to new users wearing hip exoskeletons.

To solve the above problems, we propose a fast joint moment estimation method based on general moment feature (GMF) generation. In the training phase, this method utilizes the user’s body parameters and hip joint moment to generate GMF using a feature generator. This GMF is then used to train a GRU (gated recurrent unit) neural network-based estimator, which can quickly predict the GMF. Additionally, a decoder is trained to decode the GMF into biomechanical joint moment. During the predicting phase, the trained estimator is used to rapidly estimate the GMF, which is subsequently decoded by the decoder to obtain the predicted joint moment.

The main contributions of this study are:

- 1) Proposing a GMF generation method based on body parameters, which is conducive to obtaining a more individual-independent generalized representation of biomechanical joint moments and improves the performance of the joint moment estimation model.
- 2) Developing an estimator based on GRU, which addresses the real-time requirements of lower-limb exoskeleton application by taking advantage of the characteristics of recurrent neural networks in time series data prediction.
- 3) Demonstrating the effectiveness of the proposed method through experiments with a dataset, which shows that it has higher accuracy, faster computation time than existing methods, and strong generalization capability.

The structure of this paper will be described as follows. Section II describes the proposed fast joint moment estimation method based on GMF generation. The experiments and results are presented in sections III and IV, discussed in section V. The conclusion of this paper is written in section VI.

II. METHOD

This section provides a detailed explanation of the proposed fast joint moment estimation method based on GMF generation. We will firstly describe the basic model of using neural networks to estimate biomechanical joint moment. Then we introduce the concept of GMF, addressing the issues that arise from the general form. Based on this, we propose a network architecture for generating GMF as well as a decoder for it (Fig.1 - Model training) and introduce a fast estimator using GRU neural networks. Finally, we present the training method for the neural network model and the prediction process of estimating joint moment (Fig.1 - Prediction).

A. The Basic Model of Joint Moment Estimation

This study aims to estimate the hip joint moment based on the joint kinematics during walking utilizing neural networks.

As mentioned in [24], the interpretability of a model is crucial for generating models with superior accuracy and robustness. Therefore, we first assume two essential attributes that a model should possess to estimate joint moment: 1) incorporating the relationship between kinematics and dynamics, and 2) ensuring the continuity of motion.

The rationality of the second attribute is supported by previous researches [25], [26], [27], which indicates that using an appropriate window to capture the input time series can improve the prediction accuracy of the joint estimation model. Regarding the first attribute, to determine the model inputs from candidate kinematic information, we conducted a series of preliminary experiments. Finally, we selected six-dimensional data comprising the angles, angular velocities, and angular accelerations of the bilateral hip joints as the inputs for each time step of the estimator. The results of these experiments demonstrated that as the dimensionality of the inputs increased, the predictive accuracy of the joint moment estimation model gradually improved. Therefore, the general inputs of the model can be described as follows: $\mathbf{X} = [\mathbf{x}_t, \mathbf{x}_{t-1}, \dots, \mathbf{x}_{t-\Delta T}] \in R^{\Delta T \times D}$, where ΔT represents the window size and D denotes the dimensionality of the joint kinematics data ($\Delta T = 100$, $D = 6$). A basic neural network model for estimating joint moment is described as F . For the estimated joint moment \widehat{M} at time t , the process of estimation can be expressed as:

$$\widehat{M} = F(\mathbf{X}). \quad (1)$$

B. Generation of GMF

The conventional form of joint moment estimation networks does not incorporate personalized information of the subjects. Therefore, to address the issue of decreased prediction accuracy when directly estimating joint moment using joint kinematics in a multi-user environment, we propose an estimation method based on GMF generation. Firstly, we introduce the concept of GMF, which is an individual-independent representation from the joint moment that combines with subject's body parameters (mass and height are used in this paper). Next, a generator is proposed to generate this feature. Finally, we will explain the decoding process that decodes generated GMF into joint moment.

1) *GMF*: Here, we first directly introduce the application form of GMF for joint moment estimation. According to the expression in (1), the joint moment estimation method based on GMF can be represented as follows:

$$\widehat{GMF} = E(\mathbf{X}) \quad (2)$$

$$\widehat{M} = R(\widehat{GMF}), \quad (3)$$

where E denotes the GMF estimator and R denotes the GMF decoder, satisfying $R(E(\cdot)) \in F(\cdot)$. Using the estimator to estimate the proposed GMF instead of directly estimating the joint moment, we can reduce the decrease in prediction accuracy caused by individual differences, improving the generalization performance of the joint estimation model across multiple users.

Based on the aforementioned requirements, we design a method for generating GMF and apply it to the training of the joint moment estimation model. Fig.1 illustrates the process of generating GMF. The joint moment estimation method based on GMF leverages both the joint moment and body parameters. It utilizes an adaptive neural network to extract GMF that is independent of individuals. This feature is then used to train the estimator. Additionally, a decoder is trained to decode the estimated GMF into joint moment. It is worth noting that, unlike directly inputting body parameters into the network, this method expresses the role of body parameters in the network model more specifically, which means it can achieve the optimal mapping between hip joint kinematics and joint moment.

2) *GMF Generator*: A feature generator G is used to generate the GMF. More specifically, this generator utilizes a neural network to combine the joint moment of subjects with their body parameters and finally generates the desired GMF.

The main objective of GMF generation is to discover a better prediction target to achieve a more accurate estimation by the estimator E as described by (2). Therefore, unlike typical deep learning tasks, in this method, the labels learned by the estimator and the GMF generator are mutually the output values of each other during the training process. This structure guides the GMF generator to generate training labels, namely the proposed GMF, from the joint moment and body parameters of subjects, which can enhance the accuracy of the estimator.

At the same time, it is notable that the GMF generated by the generator should have the capability to be decoded into joint moment. Using θ_G to represent the network parameters of the feature generator G , Q and M to represent the values of the subject's body parameters and joint moment, respectively ($Q = [m, h]$), the process of generating GMF can be expressed as follows:

$$GMF = G(Q, M; \theta_G). \quad (4)$$

The optimal generator parameters θ_G^* in the above process can be mathematically represented as:

$$\theta_G^* = \underset{\theta_G}{\operatorname{argmin}} \|E(\mathbf{X}; \theta_E) - G(Q, M; \theta_G)\|_2 \quad (5)$$

s.t. $G(\theta_G) \in S(\theta_S)$,

where S represents the function space in which G resides, ensuring the GMF generated through G can be decoded into joint moment.

The network structure of training phase (as shown in Fig. 1) provides a specific illustration of the role of the GMF generator within the overall network structure. The inputs of the generator include joint moment and body parameters, and its output is the GMF. The GMF Generator serves two important functions: a) generating the optimal GMF to improve the prediction accuracy of the estimator, enhancing the model's performance across different users; b) ensuring the decoder to accurately decode the generated GMF into joint moment.

To implement an model with the proposed method, as an example, we employ a fully connected network with five hidden layers to construct the GMF generator. Each hidden

layer consists of 32 nodes, and LeakyReLU activation function is applied after each hidden layer to introduce non-linearity.

3) *GMF Decoder*: The GMF decoder is used to decode the generated GMF into joint moment. We employ the same network structure as the GMF generator for constructing the GMF decoder. To improve the accuracy of the output, we include body parameters as part of its inputs. Using \mathbf{R} to represent the moment decoder, $\theta_{\mathbf{R}}$ as its network parameters, and \widehat{M} as the decoded joint moment values, the process of joint moment decoding can be expressed as:

$$\widehat{M} = \mathbf{R}(Q, GMF; \theta_{\mathbf{R}}). \quad (6)$$

The optimal parameters $\theta_{\mathbf{R}}^*$ of the GMF decoder in the above process can be obtained from:

$$\theta_{\mathbf{R}}^* = \underset{\theta_{\mathbf{R}}}{\operatorname{argmin}} \|\mathbf{R}(Q, GMF; \theta_{\mathbf{R}}) - M\|_2. \quad (7)$$

C. GMF Estimator

To ensure the efficiency of the model, we design the GMF estimator with more consideration to the computational efficiency of the network, using a GRU neural network.

Since the inputs (\mathbf{X}) and outputs (\widehat{GMF}) of the model in this study are both time series, joint moment estimation is essentially a time series regression problem. In such problems, recurrent neural networks have demonstrated high accuracy [28]. In the designed exoskeleton system, these networks can better leverage their ability to estimate joint moment in real-time. Based on the characteristic of memory information propagation, the network only needs to inherit the hidden state information from the previous time step and input the features of the current time step during real-time computation. Therefore, the inputs of the model can be redefined as: $\mathbf{X}_t = [\mathbf{x}_t, \mathbf{H}_t] \in R^{2 \times D}$ (ideally, $[\mathbf{x}_t, \mathbf{H}_t] \equiv [\mathbf{x}_t, \mathbf{x}_{t-1}, \dots, \mathbf{x}_{t-\Delta T}]$). The relationships between each time step are explicitly expressed without the need for internal processing within the network, which significantly reduces the number of network parameters.

Existing recurrent neural network structures include RNN, LSTM, GRU [29]. Due to the challenges of RNN in handling long-term dependencies, vanishing gradients, and exploding gradients, they have been gradually replaced by LSTM and GRU. Furthermore, GRU has a more simplified structure and fewer parameters compared to LSTM, resulting in lower memory usage and faster execution. In many cases, there is no significant difference in prediction accuracy between the two models [30]. Therefore, the estimator in this study utilizes a neural network based on the GRU structure.

In this study, only one GRU block is used as an implementation case, with 16 hidden neurons, and a fully connected network with a size of 16*1 is used to output the predicted target (Fig. 2). Specifically, at each time step, the GRU receives two different modalities: the hidden information from the previous time step's GRU hidden layer and the inputs \mathbf{X} . It adjusts the information flow through update gates and reset gates, and finally obtains the output based on these two gates. Thus, given the hip joint sagittal plane angle signal at time t as \mathbf{X}_t , the hidden inputs from the previous time step as

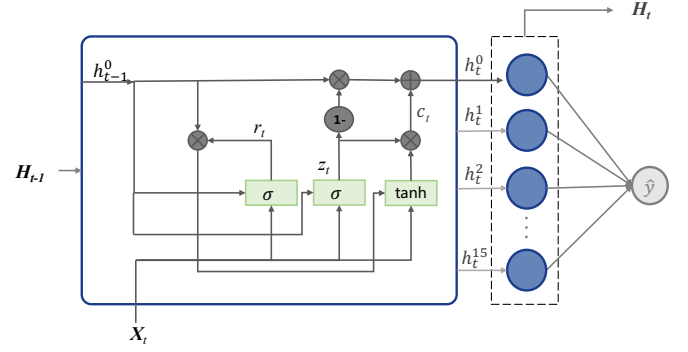


Fig. 2. The fast estimator based on GRU, the computation process of one output within the GRU unit, denoted as h^0 , is shown in the solid box. The computation process for the remaining 15 hidden layer nodes, inputs ($h_{t-1}^1 - h_{t-1}^{15}$), and outputs ($h_t^1 - h_t^{15}$), follows the same process.

\mathbf{H}_{t-1} , the estimated GMF at the current time step \widehat{GMF} can be obtained as follows:

$$\mathbf{R}_t = \sigma(\mathbf{W}_{xr}\mathbf{X}_t + \mathbf{W}_{hr}\mathbf{H}_{t-1} + \mathbf{b}_r) \quad (8)$$

$$\mathbf{Z}_t = \sigma(\mathbf{W}_{xz}\mathbf{X}_t + \mathbf{W}_{hz}\mathbf{H}_{t-1} + \mathbf{b}_z) \quad (9)$$

$$\mathbf{C}_t = \tanh(\mathbf{W}_{xc}\mathbf{X}_t + \mathbf{W}_{hc}(\mathbf{R}_t \odot \mathbf{H}_{t-1}) + \mathbf{b}_c) \quad (10)$$

$$\mathbf{H}_t = (1 - \mathbf{Z}_t) \odot \mathbf{H}_{t-1} + \mathbf{Z}_t \odot \mathbf{C}_t \quad (11)$$

$$\widehat{GMF} = \mathbf{W}_{FC}\mathbf{H}_t + \mathbf{b}_{FC}, \quad (12)$$

where \mathbf{W}_{xr} , \mathbf{W}_{hr} , \mathbf{W}_{xz} , \mathbf{W}_{hz} , \mathbf{W}_{xc} and \mathbf{W}_{hc} are the GRU layer weights, \mathbf{b}_r , \mathbf{b}_z and \mathbf{b}_c are biases, \mathbf{R}_t and \mathbf{Z}_t denote vectors for the activation values of the update gate and reset gate, and \mathbf{W}_{fc} is the full connected layer weights and \mathbf{b}_{fc} is the biases. Writing the network parameters (\mathbf{W} and \mathbf{b}) as $\theta_{\mathbf{E}}$, like (5), the optimal parameters $\theta_{\mathbf{E}}^*$ are solved as:

$$\theta_{\mathbf{E}}^* = \underset{\theta_{\mathbf{E}}}{\operatorname{argmin}} \|E(\mathbf{X}; \theta_{\mathbf{E}}) - G(Q, M; \theta_G)\|_2. \quad (13)$$

D. Model Training

The proposed method consists of two parts: GMF estimation and GMF decoding, which involves the training of three models: estimator, generator, and decoder. In the first part, the GMF generator is jointly trained with the estimator to obtain better individual-independent representation (GMF) and its prediction model (estimator). Meanwhile, in the second part, the GMF generator is trained together with the decoder to ensure the decodability of the generalized GMF and to obtain a model capable of decoding GMF into joint moment.

Based on (5), (7), and (13), two loss functions L_1 , L_2 are constructed for the network. The backpropagation process is shown in Fig. 1 - Model training with solid lines. L_1 represents the loss between the results of the GMF estimator and the GMF generator, while L_2 represents the loss between the outputs of the GMF decoder and ground-truth values of joint moment.

$$J_{mse}(y_i, \hat{y}_i) = \frac{1}{N} \sum_{i=1}^N (y_i - \hat{y}_i)^2 \quad (14)$$

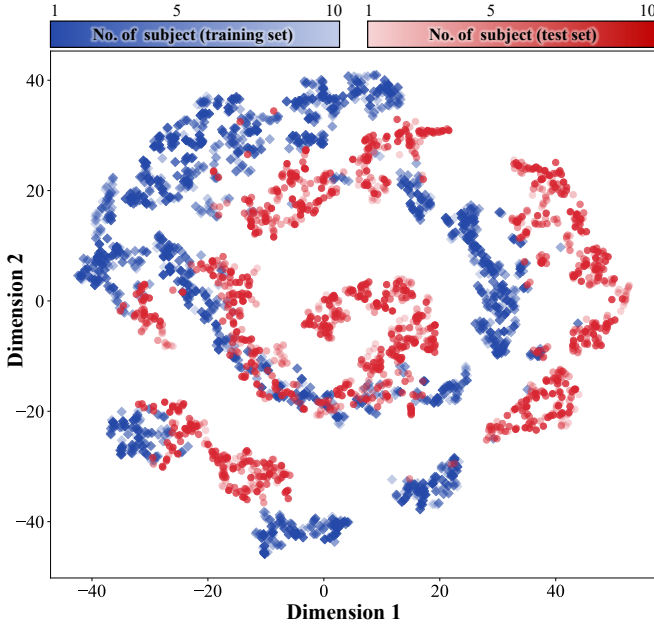


Fig. 3. Visualization of the input features distribution (joint kinematics) of the training set (in blue) and the test set data (in red) using the T-SNE method. The varying shades of color represent data from 10 individual subjects in each set. Under the data partitioning method that maximizes individual differences, the intra-subject distribution of input features within the same set (intra-class distance) appears to be similar, while the distribution of input features between different sets (inter-class distance) exhibits significant differences.

$$L_1 = J_{mse}(\mathbf{F}(\mathbf{X}), \mathbf{G}(\mathbf{Q}, M)) \quad (15)$$

$$L_2 = J_{mse}(\mathbf{R}(\mathbf{G}(\mathbf{Q}, M), \mathbf{Q}), M). \quad (16)$$

It is worth noting that the optimization of the parameters of the GMF generator are included in L_2 . By selecting the weighting coefficients w_1 and w_2 of the two loss functions, it can be ensured that the GMF, which is generated by the feature generator optimized by L_1 , can be decoded into joint moment through the GMF decoder. Therefore, the condition in (5) is satisfied. The overall loss function of the joint moment estimation network is given by:

$$Loss = w_1 * L_1 + w_2 * L_2. \quad (17)$$

E. Model Prediction

The trained GMF estimator and decoder will be used in the prediction process for the final joint moment estimation. As shown in Fig. 1 - Prediction, using the joint kinematics as input, the GMF is obtained by the fast GMF estimator, which is then combined with user body parameters to be decoded into the predicted joint moment:

$$\widehat{M} = \mathbf{R}(\mathbf{E}(\mathbf{X}), \mathbf{Q}) \quad (18)$$

III. EXPERIMENT

A. Dataset and Training-testing Data Partitioning

The publicly available dataset used in this article is sourced from [31]. The treadmill data of 20 healthy subjects (12 males

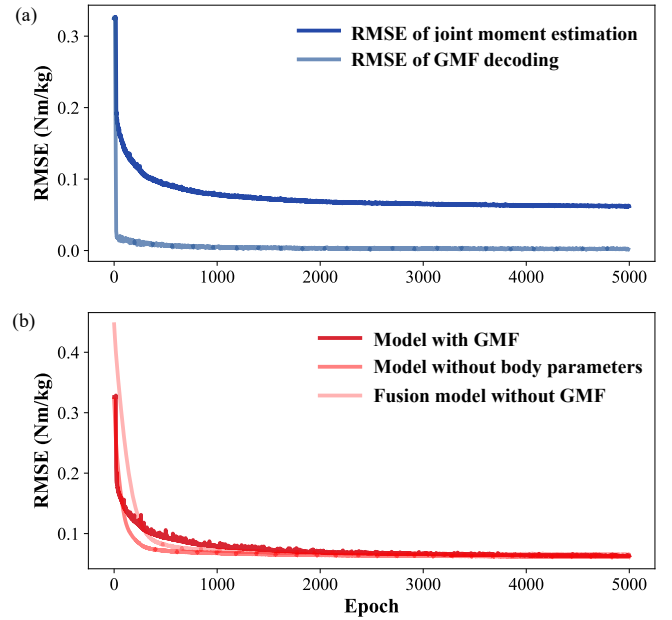


Fig. 4. (a) Trend of accuracy of the joint moment prediction (dark blue) and accuracy of GMF decoding (light blue) of training data during the training process of the proposed estimation model based on GMF. Both values of them continuously improve and converge to the optimum over the 5000 epochs. (b) Trend of prediction accuracy on the validation set for our method (dark red) compared to two other contrastive methods (light red). The three methods approximate the best accuracy achieved under the experimental conditions set.

and 8 females, age 21.20 ± 3.04 yr, height 1.70 ± 0.07 m, weight 67.76 ± 11.64 kg) were used for model training and testing. Specifically, the data of each subject included hip joint sagittal plane angle positions and flexion/extension joint moment at 28 different treadmill speeds. Data collection of each subject was performed through 7 experiments, with each experiment consisting of four different speeds maintained for 30 seconds each. The speeds for the first experiment were 0.5 m/s, 1.2 m/s, 1.55 m/s, and 0.85 m/s. In subsequent experiments, each speed increased by increments of 0.05 m/s. Hip joint angular velocity and angular acceleration were computed corresponding to the data collection frequency, and the hip joint moments used were smoothed using butterworth filtering.

To demonstrate the effectiveness of the proposed method, the dataset was partitioned based on inter-subject differences to create a maximum separation between training and test data, resembling a multi-user scenario. The T-SNE method was utilized to divide the hip joint angle data samples from the subjects into two categories, as shown in Fig. 3, with 10 subjects in each category. Consequently, for the experiments in this study, the training and validation sets were composed of data from the first 10 subjects (in an 8:2 ratio, independent of each other), while the data from the remaining 10 subjects were used as the test set to assess the model's performance.

B. Implementation Details

We conducted model training on a device with an Intel CPU (Core i7-12700F) and an Nvidia GPU (GeForce RTX 3060Ti).

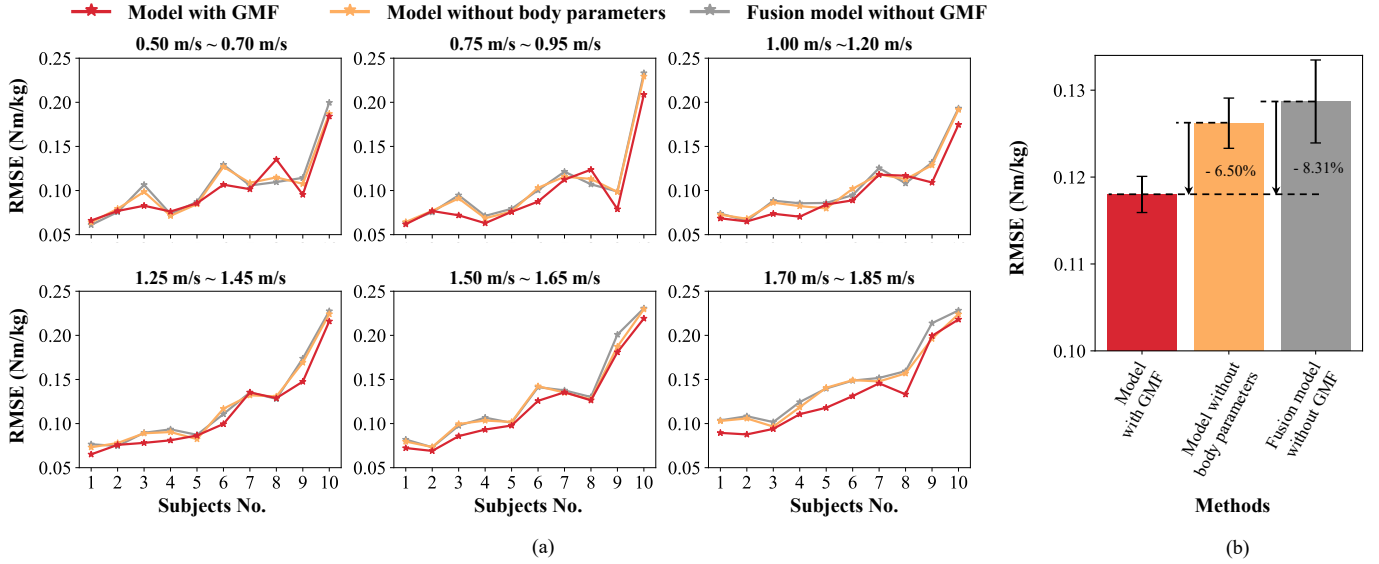


Fig. 5. (a) Comparison of the accuracy of joint moment estimation for all subjects at different speed ranges using the proposed method, along with the baseline methods. The proposed method improves the prediction accuracy of the model in most cases, especially at faster speeds. (b) Comparison of the overall average and variance of the test results for the three methods.

The Adam optimizer [32] was employed. In all experiments, we performed five repetitions with different random initializations to ensure robustness. Detailed parameters are described in each section before the corresponding experiment results.

IV. RESULTS

In this section, we first present the convergence of the proposed model during training in section A. Sections B and C respectively demonstrate the accuracy improvement brought by the proposed joint moment estimation method and the computation speed improvement achieved by using a GRU-based estimator. In section D, we further show the generalization performance of GMF.

A. Convergence of Neural Network

The convergence of the proposed neural network trained with 10 subjects is illustrated in Fig. 4 (a), represented by the root mean square error (RMSE):

$$RMSE = \sqrt{\frac{1}{n} \sum_{i=1}^n (y_i - \hat{y}_i)^2}, \quad (19)$$

where \hat{y}_i denotes the estimated value by the neural network, y_i is the ground truth value, and n is the number of samples. During the training process, both the joint moment prediction accuracy and the decoding accuracy of the decoder consistently improved without significant fluctuations. The RMSE of the joint moment estimation on the training dataset, averaged over five repetitions, was 0.0630 ± 0.0014 Nm/kg, while the RMSE of GMF decoding was 0.0016 ± 0.0017 Nm/kg.

B. Estimation Accuracy of Models

We evaluated the performance of the proposed method by computing the RMSE of the predicted joint moment on the

test dataset. To better demonstrate the effectiveness of the proposed method, we compared our method with two baseline methods: 1) without body parameters, which means directly estimating moment by inputting joint kinematics into the estimator; 2) conventional body parameters fusion model without GMF, which means implementing a fusion model where two networks separately take joint kinematics and body parameters as inputs to obtain two hidden features, and these two features are then stacked and passed through a fully connected network to estimate joint moment. To ensure comparability, the architecture of the estimator inputting joint kinematics is the same for all three baseline models, and the optimizer (Adam) parameters and initial learning rate ($lr = 0.001$) are the same. In our method, we set the parameters $w_1 = 1$ and $w_2 = 0.05$ in (17).

Fig. 5 reports the RMSE results of our method compared to the baseline methods. Overall, our method achieves an RMSE of 0.1180 ± 0.0021 Nm/kg on the test dataset. The mean results show a significant improvement compared to the two baseline methods (6.50% vs. baseline method 1 and 8.31% vs. baseline method 2). The experimental results demonstrate that, except for subject 6, whose average joint moment estimation error increased by 0.97% compared to baseline method 1 and 2.57% compared to baseline method 2, the joint moment estimations for other subjects are more accurate. The baseline method 2, which directly fuses body parameters (Q) and joint kinematics (X) through the network, does not achieve improved joint moment estimation accuracy compared to baseline method 1 with only inputting joint kinematics. In fact, there is even a decrease, indicating that it is challenging to achieve body parameter fusion using conventional fusion models.

As it is difficult to achieve the optimal validation set accuracy with limited time, in addition to using the RMSE, we used the rate of increase in the RMSE on the test set relative

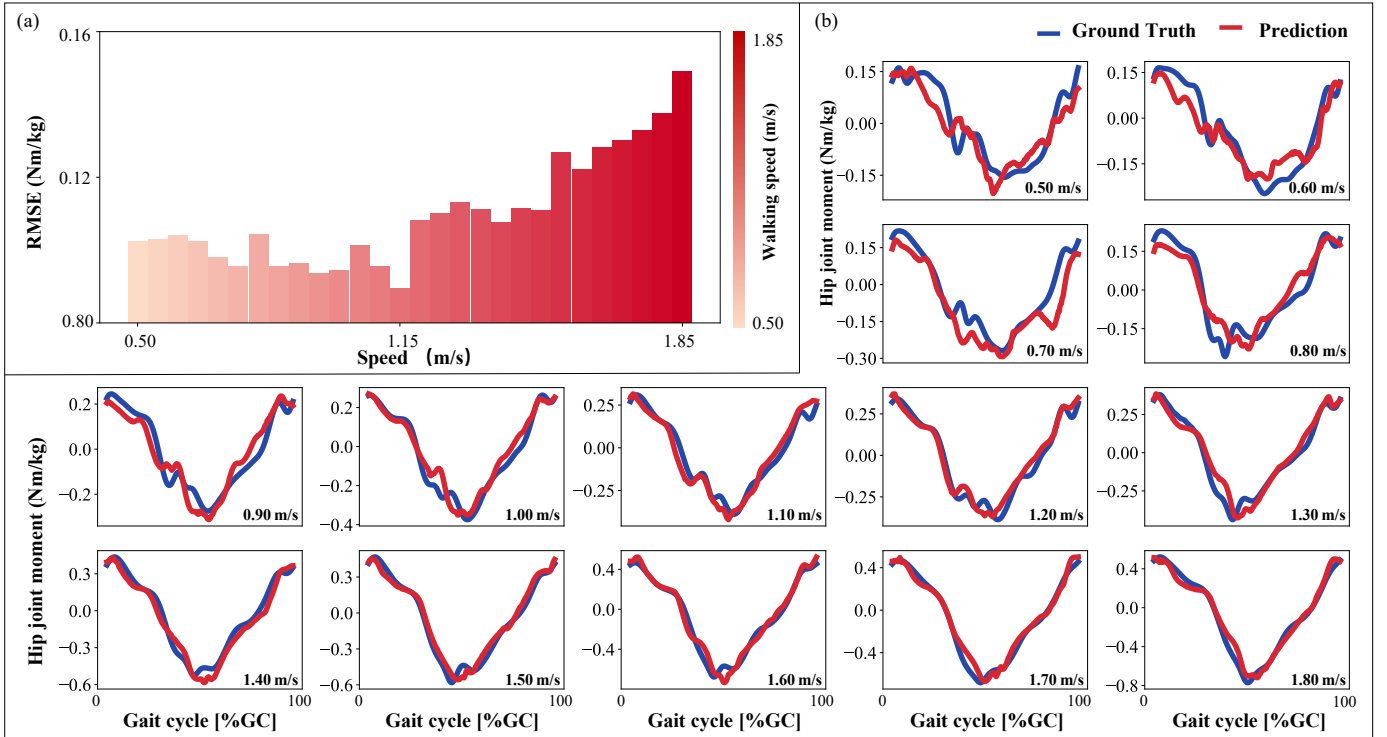


Fig. 6. (a) Joint moment estimation error of the proposed method at 28 different walking speeds. The results show that within the provided range of walking speeds, the joint moment estimation error exhibits a “V” shaped pattern, with the minimum estimation error occurring at 1.15 m/s. (b) Samples of the predicted curve and the ground truth curve of a complete gait cycle for one subject at 14 walking speeds, spaced at intervals of 0.1 m/s.

TABLE I
 R_{tv} OF PROPOSED METHOD COMPARED TO 2 BASELINE METHOD

	Ours	Baseline 1	Baseline 2
R_{tv}	0.8907	1.1142	1.1023
Rate of Increase	-	20.06%	19.20%

to the RMSE on the validation set (R_{tv}), which represents the degree of overfitting of the optimal model, obtained from:

$$R_{tv} = \frac{RMSE_{test} - RMSE_{validation}}{RMSE_{validation}}. \quad (20)$$

This equation implies that the R_{tv} of a model with better generalization performance should be smaller (with consistent accuracy on the validation dataset).

Fig.4 (b) shows the variation of validation accuracy during the training process for our method and the two baseline methods. All three models achieve similar accuracy on the validation set (around 0.0632 Nm/kg). Based on the statistical analysis (Table. I), our method reduces R_{tv} by 20.06% and 19.20%. While RMSE intuitively demonstrates the effectiveness of our method, the R_{tv} for result evaluation reveals the underlying reason for the accuracy improvement of our method: the mapping of GMF and joint kinematics is more accurate, reducing the prediction inaccuracy of the model in new subject environments.

A complete hip joint moment curve for one gait cycle of a subject at 14 different walking speeds is shown in Fig. 6 (b) for qualitative comparison between the ground truth and predicted values. Furthermore, we analyzed the variation of

model estimation error across 28 walking speeds ranging from 0.5 m/s to 1.85 m/s, as depicted in Fig. 6 (a). The estimation error exhibits a decreasing and then increasing trend. For low walking speeds, this could be attributed to the greater variability in gait patterns during slowly walking [33]. On the other hand, the increase in estimation error for fast walking speeds is likely driven by the higher magnitude of joint moments. If statistical analysis is performed using normalized metrics such as normalized root mean squared error (NRMSE), it can be observed that the estimation errors for high walking speeds do not always increase but even decrease compared to moderate walking speeds.

C. Computation Time of Models

To evaluate the performance of the proposed GRU-based estimator in terms of computation time, experiments were conducted on it as well as four existing mainstream network structures(as shown in Fig. 7) for 20 rounds of 10,000 joint moment estimations. All models maintained the structure of the estimator-decoder in the prediction part of Fig. 1.

Previous studies such as [23], [26], [27] have demonstrated that increasing the number of network parameters has a positive impact on the prediction accuracy of joint moment estimation. Therefore, to ensure comparability of the experimental results, we adjusted the network parameter number of the four models to make them as close as possible to the GRU-based model in terms of validation accuracy. Due to device and time limitations, we found it difficult to adjust the TCN to the ideal accuracy, and its optimal validation accuracy was slightly

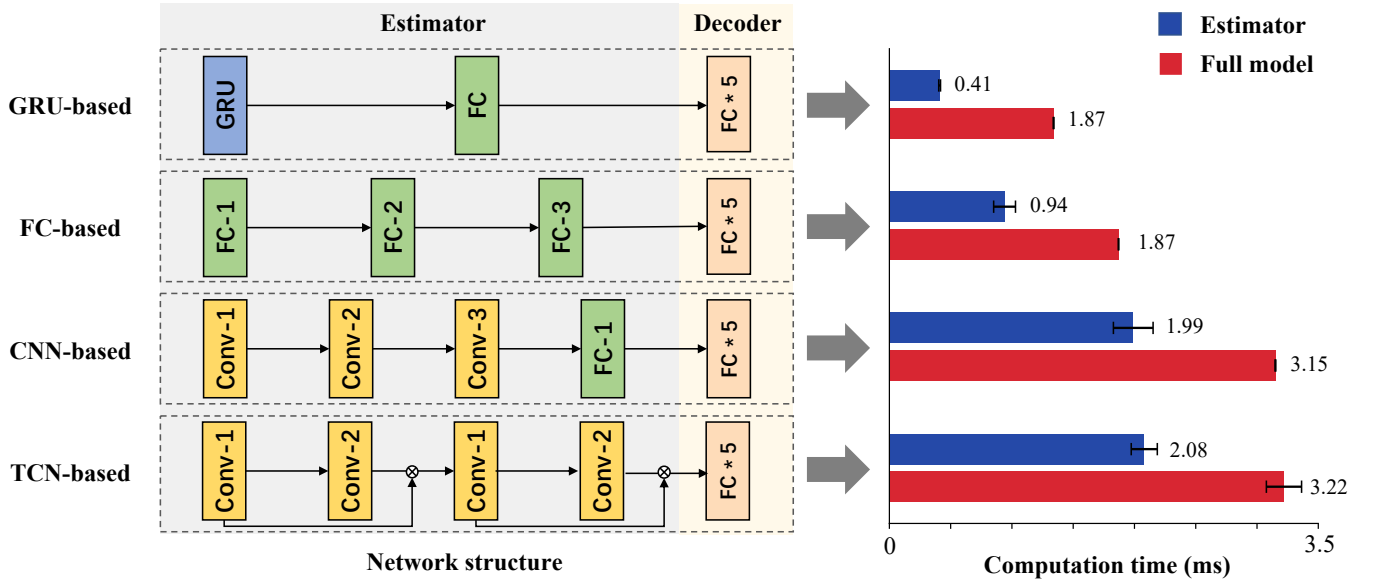


Fig. 7. Four joint moment prediction models consisting of estimators with different neural network structures (left), including the proposed GRU-based method for fast estimation and three mainstream model architectures. Average computation time required for a single calculation for each model (right). The blue bar represents the computation time for the GMF estimator, while the red bar represents the total computation time for the joint moment estimation model, including the GMF estimator and decoder.

TABLE II
NET STRUCTURE PARAMETERS DESCRIPTION

GRU-based	Hidden num: 16
	Layer num: 1
Full Connected Layer: 16,1	
FC-based	Layer 1 node num: 32
	Layer 2 node num: 16
	Layer 3 node num: 16
CNN-based	Conv1: kernel 3*1, padding 1, channel 32
	Conv2: kernel 3*1, padding 1, channel 64
	Conv3: kernel 3*1, padding 1, channel 32
	Adaptive Average Pooling: output size 1
	Full Connected Layer: 32,1
TCN-based	Residual block num: 2
	Conv1 in block: kernel 3*1, padding 1, dilation 1
	Conv2 in block: kernel 3*1, padding 2, dilation 2

higher than the other networks, indicating that its parameter size needs to be further increased. Therefore, the joint moment estimation time of the TCN network under this experimental condition may be longer. The network parameters used in the experiments are shown in Table. II.

Fig. 7 depicts the computation time of joint moment estimation models based on four estimators. When the input length is 100 time steps, the model with GRU-based estimator demonstrates significantly higher computational efficiency compared to the others. In comparison to estimators with FFN, CNN, and TCN, the computation speed of joint moment estimation is improved by 28.34%, 57.46%, and 58.39% respectively. This result indicates that in scenarios where real-time requirements need to be satisfied, such as in exoskeleton-assisted applications, the model structure based on recurrent neural networks like GRU-based networks have greater potential.

D. Generalization of GMF

To verify the generalization of the proposed GMF, the three models with different estimators mentioned in computation time comparison experiment were further used to observe the changes in joint moment estimation accuracy after introducing GMF, following the experimental process outlined in section III-B.

A pre-trained joint moment estimation model with GRU-based estimator was selected for this experimentation. Based on the selected model, we replaced the GRU-based estimator with three estimators with different network structures. Following the training process shown in Fig. 1, a series of new training processes were conducted. During the training process, only the parameters of the new estimator were updated while the parameters of the generator and decoder were fixed (keeping the generated GMF unchanged).

Table. III presents the performance of GMF in the generalization experiment. Within the scope of this experiment, all four estimators showed an improvement in joint moment estimation accuracy after introducing GMF (compared to the method without body parameters: 7.96% in FFN, 8.12% in CNN, 8.41% in TCN, and compared to the method fusion body parameters but without GMF: 11.44% in FFN, 10.94% in CNN, 9.13% in TCN). Since the GMF generator and decoder used in the experiment were from a pre-trained model and with no parameters change, the results further demonstrate that the generated GMF is a more individual-independent representation of joint moment and contributes to the accuracy of predicting joint moment based on joint kinematics.

V. DISCUSSION

This study utilizes a GMF generation method with GRU-based network to achieve a better estimation of hip joint

TABLE III
COMPARISON OF THE PREDICTION ACCURACY OF THE MODEL WITH THE GMF AND THE MODELS WITHOUT THE GMF

Model	Model without body parameters	Fusion model without GMF	Ours
GRU	0.1262±0.0021	0.1287±0.0048	0.1180±0.0030
FFN	0.1270±0.0029	0.1324±0.0048	0.1169±0.0018
CNN	0.1231±0.0009	0.1270±0.0122	0.1131±0.0009
TCN	0.1260±0.0011	0.1270±0.0037	0.1154±0.0008
Average	0.1256±0.0015	0.1288±0.0022	0.1159±0.0018

moment. To the best of our knowledge, this is the first study that considers real-time and inter-user variability issues in joint moment estimation and proposes a solution. On one hand, we demonstrate the real-time value of GRU-based neural networks in joint moment estimation. On the other hand, the GMF, which is obtained through an adaptive neural network, leads to significant improvements in model accuracy and has the potential to become an advanced method for future joint moment estimation and analysis.

A. The Inputs of the Model

Compared to most existing methods for estimating joint moment (using sensor information such as IMU and EMG as input to train the model), the GRU-based estimator used in this paper takes 6-dimensional joint kinematics data as inputs instead of sensor data. This is because the joint moment estimation is considered a model identification problem that requires establishing an approximate model with dynamic characteristics rather than a completely uninterpretable black-box model. For practical applications, model training can be performed using angles obtained from sensors or using highly correlated data of sensors as inputs directly, without requiring changes to the overall model structure. However, additional challenges may be posed in these ways such as sensor accuracy drift and data loss.

Other inputs used by the model are human body parameters, which are composed of height and weight in this paper. These two parameters may not be the optimal inputs for obtaining GMF. Future research could explore more suitable body parameters to achieve better GMF generation and more accurate predictions in the problem of joint moment estimation based on joint kinematics.

B. Accuracy of the Decoder

To decode the GMF, we use a fully connected neural network of which the structure is the same as the feature generator, and make the loss of decoder back-propagate to the generator with a weighting coefficient to ensure the decodability of the generated GMF. While this method achieves high accuracy (decoding RMSE less than 0.003 Nm/kg) in decoding the GMF into joint moment, the decoding error can only approximate zero rather than reaching it due to the use of a separate neural network. Additionally, to ensure the accuracy of GMF decoding, the decoder may become overly complex, spending extra computation time. This turns what seems like a simple inverse transformation task into a complex and inaccurate one. The concept of reversible neural networks [34],

[35], [36], which have lightweight memory consumption and can preserve input information features, has been proposed. When applied to our method, it has the potential to achieve zero error in GMF decoding with fewer parameters. We may further explore the application of such networks in our method in the future.

C. Time Efficiency Consideration

When comparing the timeliness of estimators, the experimental results shown in this study using a python environment on the same device have clear significance in terms of the relative computation time of the models. However, the absolute values of computation time for each model cannot directly represent the actual computation speed when applied to exoskeletons. To achieve quick response exoskeleton control, methods such as model compression and deployment with C/C++ language are necessary.

Since the proposed method originates from the research on assistive hip exoskeleton control, the estimator model proposed in this paper uses a GRU-based network structure. However, for joint moment estimation tasks that do not require timeliness, the optimal network structure for the estimator may not necessarily be based on recurrent neural networks. The joint moment estimation method we propose can be extended to the field of biomechanics, as demonstrated in the generalization experiment, where it also performs well on mainstream neural networks besides the GRU-based network. For systems that have low real-time requirements, future researchers can use more appropriate network structures within the framework of this method to obtain higher-precision joint moment estimation models.

VI. CONCLUSION

To address the issues of long computation time and lack of personalization in neural networks used for fast joint moment estimation, this study proposes an estimation method based on GMF generation. The method utilizes a generator to adaptively generate GMF, which serves as a more individual-independent representation compared to the biomechanical joint moment. A GRU-based neural network is then employed to predict the generated GMF. The GMF improves the prediction accuracy of the estimator while being decoded into joint moments accurately. Additionally, the GRU-based estimator demonstrates the capability to quickly estimate GMF. Experimental results on prediction accuracy and computation time of the joint moment estimation model validate the effectiveness of the proposed method. In particular, the generalization experiment

demonstrates that this method can be applied to various neural networks structure for joint moment estimation, which means it has potential to achieve better accuracy with more refined adjustments to the network structure. The contributions of this work enable better implementation of real-world joint moment estimation and its application in guiding exoskeleton control.

REFERENCES

- [1] W. Cao, C. Chen, D. Wang, X. Wu, L. Chen, T. Xu, and J. Liu, "A Lower Limb Exoskeleton With Rigid and Soft Structure for Loaded Walking Assistance," *IEEE Robotics and Automation Letters*, vol. 7, no. 1, pp. 454–461, Jan. 2022.
- [2] D. J. Hyun, H. Park, T. Ha, S. Park, and K. Jung, "Biomechanical design of an agile, electricity-powered lower-limb exoskeleton for weight-bearing assistance," *Robotics and Autonomous Systems*, vol. 95, pp. 181–195, Sep. 2017.
- [3] B. Kalita, J. Narayan, and S. K. Dwivedy, "Development of Active Lower Limb Robotic-Based Orthosis and Exoskeleton Devices: A Systematic Review," *International Journal of Social Robotics*, vol. 13, no. 4, pp. 775–793, Jul. 2021.
- [4] A. Kapsalyamov, P. K. Jamwal, S. Hussain, and M. H. Ghayesh, "State of the Art Lower Limb Robotic Exoskeletons for Elderly Assistance," *IEEE Access*, vol. 7, pp. 95 075–95 086, 2019.
- [5] R. L. Medrano, E. J. Rouse, and G. C. Thomas, "Biological Joint Loading and Exoskeleton Design," *IEEE Transactions on Medical Robotics and Bionics*, vol. 3, no. 3, pp. 847–851, Aug. 2021.
- [6] D. J. Farris and G. S. Sawicki, "The mechanics and energetics of human walking and running: A joint level perspective," *Journal of The Royal Society Interface*, vol. 9, no. 66, pp. 110–118, Jan. 2012.
- [7] J. Kim, G. Lee, R. Heimgartner, D. Arumukhom Revi, N. Karavas, D. Nathanson, I. Galiana, A. Eckert-Erdheim, P. Murphy, D. Perry, N. Menard, D. K. Choe, P. Malcolm, and C. J. Walsh, "Reducing the metabolic rate of walking and running with a versatile, portable exosuit," *Science*, vol. 365, no. 6454, pp. 668–672, Aug. 2019.
- [8] T. Xue, Z. Wang, T. Zhang, and M. Zhang, "Adaptive Oscillator-Based Robust Control for Flexible Hip Assistive Exoskeleton," *IEEE Robotics and Automation Letters*, vol. 4, no. 4, pp. 3318–3323, Oct. 2019.
- [9] Y. Qian, H. Yu, and C. Fu, "Adaptive Oscillator-Based Assistive Torque Control for Gait Asymmetry Correction With a nSEA-Driven Hip Exoskeleton," *IEEE Transactions on Neural Systems and Rehabilitation Engineering*, vol. 30, pp. 2906–2915, 2022.
- [10] K. Seo, K. Kim, Y. J. Park, J.-K. Cho, J. Lee, B. Choi, B. Lim, Y. Lee, and Y. Shim, "Adaptive Oscillator-Based Control for Active Lower-Limb Exoskeleton and its Metabolic Impact," in *2018 IEEE International Conference on Robotics and Automation (ICRA)*. Brisbane, QLD: IEEE, May 2018, pp. 6752–6758.
- [11] B. Lim, J. Lee, J. Jang, K. Kim, Y. J. Park, K. Seo, and Y. Shim, "Delayed Output Feedback Control for Gait Assistance With a Robotic Hip Exoskeleton," *IEEE Transactions on Robotics*, vol. 35, no. 4, pp. 1055–1062, Aug. 2019.
- [12] J. Zhang, C. C. Cheah, and S. H. Collins, "Experimental comparison of torque control methods on an ankle exoskeleton during human walking," in *2015 IEEE International Conference on Robotics and Automation (ICRA)*. Seattle, WA, USA: IEEE, May 2015, pp. 5584–5589.
- [13] G. M. Gasparri, J. Luque, and Z. F. Lerner, "Proportional Joint-Moment Control for Instantaneously Adaptive Ankle Exoskeleton Assistance," *IEEE Transactions on Neural Systems and Rehabilitation Engineering*, vol. 27, no. 4, pp. 751–759, Apr. 2019.
- [14] T. S. Buchanan, D. G. Lloyd, K. Manal, and T. F. Besier, "Estimation of Muscle Forces and Joint Moments Using a Forward-Inverse Dynamics Model," *Medicine & Science in Sports & Exercise*, vol. 37, no. 11, pp. 1911–1916, Nov. 2005.
- [15] S. S. P. A. Bishe, T. Nguyen, Y. Fang, and Z. F. Lerner, "Adaptive Ankle Exoskeleton Control: Validation Across Diverse Walking Conditions," *IEEE Transactions on Medical Robotics and Bionics*, vol. 3, no. 3, pp. 801–812, Aug. 2021.
- [16] R. B. D. Joshi and D. Joshi, "MoveNet: A Deep Neural Network for Joint Profile Prediction Across Variable Walking Speeds and Slopes," *IEEE Transactions on Instrumentation and Measurement*, vol. 70, pp. 1–11, 2021.
- [17] M. Mundt, W. Thomsen, T. Witter, A. Koeppel, S. David, F. Bamer, W. Potthast, and B. Markert, "Prediction of lower limb joint angles and moments during gait using artificial neural networks," *Medical & Biological Engineering & Computing*, vol. 58, no. 1, pp. 211–225, Jan. 2020.
- [18] Y. Qian, Y. Wang, C. Chen, J. Xiong, Y. Leng, H. Yu, and C. Fu, "Predictive Locomotion Mode Recognition and Accurate Gait Phase Estimation for Hip Exoskeleton on Various Terrains," *IEEE Robotics and Automation Letters*, vol. 7, no. 3, pp. 6439–6446, Jul. 2022.
- [19] J. Zhang, Y. Zhao, T. Bao, Z. Li, K. Qian, A. F. Frangi, S. Q. Xie, and Z.-Q. Zhang, "Boosting Personalised Musculoskeletal Modelling with Physics-informed Knowledge Transfer," *IEEE Transactions on Instrumentation and Measurement*, pp. 1–1, 2022.
- [20] C. Wang, P. P. K. Chan, B. M. F. Lam, S. Wang, J. H. Zhang, Z. Y. S. Chan, R. H. M. Chan, K. K. W. Ho, and R. T. H. Cheung, "Real-Time Estimation of Knee Adduction Moment for Gait Retraining in Patients With Knee Osteoarthritis," *IEEE Transactions on Neural Systems and Rehabilitation Engineering*, vol. 28, no. 4, pp. 888–894, Apr. 2020.
- [21] D. D. Molinaro, I. Kang, J. Camargo, M. C. Gombolay, and A. J. Young, "Subject-Independent, Biological Hip Moment Estimation During Multimodal Overground Ambulation Using Deep Learning," *IEEE Transactions on Medical Robotics and Bionics*, vol. 4, no. 1, pp. 219–229, Feb. 2022.
- [22] D. D. Molinaro, I. Kang, and A. J. Young, "Estimating human joint moments unifies exoskeleton control, reducing user effort," *Science Robotics*, vol. 9, no. 88, p. eadi8852, Mar. 2024.
- [23] M. S. B. Hossain, Z. Guo, and H. Choi, "Estimation of Lower Extremity Joint Moments and 3D Ground Reaction Forces Using IMU Sensors in Multiple Walking Conditions: A Deep Learning Approach," *IEEE Journal of Biomedical and Health Informatics*, vol. 27, no. 6, pp. 2829–2840, Jun. 2023.
- [24] Y. Zhang, P. Tino, A. Leonardis, and K. Tang, "A Survey on Neural Network Interpretability," *IEEE Transactions on Emerging Topics in Computational Intelligence*, vol. 5, no. 5, pp. 726–742, Oct. 2021.
- [25] M. Eslamy and M. Rastgaar, "Multi-Joint Leg Moment Estimation During Walking Using Thigh or Shank Angles," *IEEE Transactions on Neural Systems and Rehabilitation Engineering*, vol. 31, pp. 1108–1118, 2023.
- [26] D. D. Molinaro, E. O. Park, and A. J. Young, "Anticipation and Delayed Estimation of Sagittal Plane Human Hip Moments using Deep Learning and a Robotic Hip Exoskeleton," in *2023 IEEE International Conference on Robotics and Automation (ICRA)*. London, United Kingdom: IEEE, May 2023, pp. 12 679–12 685. [Online]. Available: <https://ieeexplore.ieee.org/document/10161286/>
- [27] Y. Zhang, J. Xiong, Y. Qian, X. Chen, Y. Guo, C. Fu, and Y. Leng, "Predict hip joint moment using cnn for hip exoskeleton control," in *International Conference on Intelligent Robotics and Applications*. Springer, 2023, pp. 200–209.
- [28] P. T. Yamak, L. Yujian, and P. K. Gadosey, "A comparison between arima, lstm, and gru for time series forecasting," in *Proceedings of the 2019 2nd international conference on algorithms, computing and artificial intelligence*, 2019, pp. 49–55.
- [29] K. Cho, B. van Merriënboer, D. Bahdanau, and Y. Bengio, "On the Properties of Neural Machine Translation: Encoder-Decoder Approaches," Oct. 2014.
- [30] J. Chung, C. Gulcehre, K. Cho, and Y. Bengio, "Empirical Evaluation of Gated Recurrent Neural Networks on Sequence Modeling," Dec. 2014.
- [31] J. Camargo, A. Ramanathan, W. Flanagan, and A. Young, "A comprehensive, open-source dataset of lower limb biomechanics in multiple conditions of stairs, ramps, and level-ground ambulation and transitions," *Journal of Biomechanics*, vol. 119, p. 110320, Apr. 2021.
- [32] D. P. Kingma and J. Ba, "Adam: A method for stochastic optimization," *arXiv preprint arXiv:1412.6980*, 2014.
- [33] H. G. Kang and J. B. Dingwell, "Separating the effects of age and walking speed on gait variability," *Gait & posture*, vol. 27, no. 4, pp. 572–577, 2008.
- [34] J.-H. Jacobsen, A. Smeulders, and E. Oyallon, "I-RevNet: Deep Invertible Networks," Feb. 2018.
- [35] A. N. Gomez, M. Ren, R. Urtasun, and R. B. Grosse, "The Reversible Residual Network: Backpropagation Without Storing Activations."
- [36] L. Dinh, D. Krueger, and Y. Bengio, "NICE: Non-linear Independent Components Estimation," Apr. 2015.